



OPEN

Induction of immunogenic cell death and enhancement of the radiation-induced immunogenicity by chrysin in melanoma cancer cells

Sevda Jafari¹, Alireza Khodaei Ardakan², Elnaz Mehdizadeh Aghdam^{3,4}, Asghar Mesbahi⁵, Soheila Montazersaheb^{1,6} & Ommoleila Molavi^{3,4,6}

Chrysin is a natural flavonoid with anti-cancer effects. Despite its beneficial effects, little information is available regarding its immunogenic cell death (ICD) properties. In this work, we hypothesized that chrysin can potentiate radiotherapy(RT)-induced immunogenicity in melanoma cell line (B16-F10). We examined the effects of chrysin alone and in combination with radiation on ICD induction in B16-F10 cells. Cell viability was assessed using an MTT assay. Cell apoptosis and calreticulin (CRT) exposure were determined using flow cytometry. Western blotting and ELISA assay were employed to examine changes in protein expression. Combination therapy exhibited a synergistic effect, with an optimum combination index of 0.66. The synergistic anti-cancer effect correlated with increased cell apoptosis in cancer cells. Compared to the untreated control, chrysin alone and in combination with RT induced higher levels of DAMPs, such as CRT, HSP70, HMGB1, and ATP. The protein expression of p-STAT3/STAT3 and PD-L1 was reduced in B16-F10 cells exposed to chrysin alone and in combination with RT. Conditioned media from B16-F10 cells exposed to mono-and combination treatments elicited IL-12 secretion in dendritic cells (DCs), inducing a Th1 response. Our findings revealed that chrysin could induce ICD and intensify the RT-induced immunogenicity.

Keywords Chrysin, Radiation, B16-F10 cells, AMPs, STAT3, PDL-1, IL-12

Cancer immunotherapy is a promising therapeutic strategy for eradicating cancer cells, particularly human melanoma. Cancer immunotherapy aims to reactivate the immune system, which is suppressed by cancer cells. The resistance of tumor cells to cell death and the escape of immunological surveillance are the most important challenges in cancer immunotherapy¹. Therapeutic success can be achieved by increasing the susceptibility of cancer cells to cell death and enhancing the immune recognition of low-immunogenic tumor cells². Immunogenic cell death (ICD) is a unique cell death that stimulates a specific anti-tumor immune response and overcomes the immunosuppressive tumor milieus. ICD is characterized by the release or exposure of damage-associated molecular patterns (DAMPs)³. DAMPs include diverse compounds such as extracellular protein fragments, oligosaccharides, peptides, nucleotides, DNA, and amino acids⁴. Calreticulin (CRT) is a well-known DAMP that generally exists in the lumen of the endoplasmic reticulum (ER). CRT is exposed in the outer layer of the plasma membrane during ER stress. CRT is one of the 'eat me' signals for phagocytosis of dying cells by dendritic cells (DCs)⁵. Another DAMPs released by tumor cells during ICD is adenosine triphosphate (ATP). Once ATP is released by dying tumor cells, it attracts more DCs to cancer sites by stimulating purinergic receptors on DCs. ATP creates a strong "find-me" signal for macrophages and DCs⁶. Heat shock proteins (HSPs) and high mobility group box 1 (HMGB1) are two other members of DAMPs released from immunogenic dying cancer cells into extracellular space and activate toll-like receptor 4 (TLR4) on DCs⁷. Upon binding to TLR4 receptors, the anti-tumorigenic Th1 response is activated which can reverse tumor-induced immunosuppressive microenvironment and facilitates the eradication of cancer cells through tumor-specific cytotoxic T cells⁸.

¹Nutrition Research Center, Tabriz University of Medical Sciences, Tabriz, Iran. ²Faculty of Veterinary Medicine, Islamic Azad University, Science and Research Branch, Tehran, Iran. ³Molecular Medicine Research Center, Tabriz University of Medical Sciences, Tabriz 51664-14766, Iran. ⁴Department of Pharmaceutical Biotechnology, Faculty of Pharmacy, Tabriz University of Medical Sciences, Tabriz 51664-14766, Iran. ⁵Medical Radiation Research Team, 84 Gorge Road, South Morang, Melbourne, Australia. ⁶These authors contributed equally: Soheila Montazersaheb and Ommoleila Molavi. [✉]email: smontazersaheb@gmail.com; montazersahebs@tbzmed.ac.ir; molavio@tbzmed.ac.ir

Radiation therapy (RT) is a cancer treatment modality capable of eliciting an immunogenic variant of regulated cell death and activating tumor-targeting immune responses⁹. Nevertheless, RT often employs high-energy radiation to ionize atoms/molecules, causing dsDNA damage and inducing ICD in cancer cells. RT directly causes DNA damage by cleaving DNA strands, leading to apoptosis and necrosis. In addition, RT exerts indirect damage by forming reactive oxygen species (ROS) that cause DNA damage. It is evident that conventional RT causes harmful impacts on the normal surrounding tissue; thereby, delivering a controlled dose of radiation is an important option in cancer therapy¹⁰. To address this issue, combination treatment regimens are being developed to optimize the synergistic effects and improve the clinical outcome of RT in cancer patients¹¹.

Recent findings have shown that ICD is triggered by specific natural agents and chemotherapeutics that activate anti-cancer immune responses^{8,12}. Chrysin is a natural compound under the class of flavonoids. Based on chemical structure, chrysin holds two phenyl rings (A and B) and one oxygen-containing heterocyclic ring. This compound has several pharmacological properties. Chrysin exerts its anti-tumor activity through JAK-STAT, MAPK, COX-2, and NF- κ B pathways^{13,14}. Chrysin mediates ROS-induced apoptotic cell death¹⁵. Moreover, a previous report showed that chrysin could act as a radiosensitizing agent and enhance apoptosis in breast cancer cells¹⁶. Indeed, chrysin reduced the expression of signal transducer and activator of transcription 3 (STAT3), which is hyperactive in most cancer cells such as melanoma and contributes to tumor-induced immunosuppression by producing immunosuppressive factors¹⁷. Emerging evidence reveals that STAT3 and programmed death ligand 1 (PD-L1) are overexpressed in melanoma and other types of cancers^{9,18}, resulting in immune escape in most cancers¹⁹. Relying on this notion, the phosphorylated STAT3 (p-STAT3) and/or PD-L1 suppression may be a potent target in cancer immunotherapy. Despite the well-known properties of chrysin, no studies have explored its role in inducing and potentiating RT-induced ICD in cancer cells. We hypothesize that the chrysin will potentiate ICD induction and improve the radiation-induced immunogenicity compared to individual treatments. Understanding the ability of chrysin to potentiate RT-induced ICD could pave the way for novel therapeutic strategies in cancer treatment, emphasizing the importance of exploring natural agents as a promising ICD-inducer compound for enhanced efficacy and reduced toxicity in clinical settings. This research advances our knowledge and underscores the translational potential of combining natural compounds and RT to improve cancer patient outcomes. For this purpose, chrysin alone and in combination with RT was used in the melanoma cell line, and DAMPs levels were determined to show how it influences the induction of ICD and enhances radiation-induced immunogenicity.

Materials and methods

Cell line and mice

B16-F10 cell line, as a melanoma model, was purchased from the Pasteur Institute of Iran (Tehran, Iran). The cells were cultivated in RPMI medium supplemented with 10% FBS and 100 U/mL penicillin/streptomycin and incubated at 37 °C with 5% CO₂. The medium was changed when it turned yellow. Upon reaching 70–80% confluence, cells were subjected to the designed treatment plan. Chrysin (Cat No: 480-40-0) was provided by Sigma (USA) and dissolved in DMSO to prepare a stock solution on the day of treatment. On the day of the experiment, a stock solution was prepared at a pre-designated concentration in the final medium. C57BL/6 female mice were purchased from the Pasteur Institute of Iran. Mice aged 9–12 weeks were used to prepare primary DCs cultures. All animal experiments were performed in accordance with guidelines published in the Guide for the Care and Use of Laboratory Animals (NIH Publication No. 8023, revised 1978). The study protocol was approved by the ethics committee at Tabriz University of Medical Sciences, Tabriz, Iran (Ethic Code No: IR.TBZMED.VCR.REC.1402.084).

Cytotoxicity assay and cell viability assay

The *in vitro* cytotoxicity of chrysin was determined using the 3-(4, 5-dimethylthiazol-2-yl)-2,5-diphenyltetrazolium bromide (MTT) assay. B16-F10 cells at a density of 0.3×10^4 were seeded in 96-well plates and then incubated overnight. To prepare chrysin stock solution, 10 mg of chrysin was dissolved in 1 mL DMSO. Different concentrations of chrysin (25, 50, 75, 100 and 125 μ M) were used to treat cells in the logarithmic phase of growth. According to the chrysin concentration, DMSO was used as a control group at a concentration of 0.06, 0.12, 0.19, 0.24, and 0.3% in MTT assay. 0.5% DMSO is considered and recommended as a safe concentration without toxicity for almost all cells²⁰. Accordingly, only untreated cells served as the control group in the following combination therapy experiments. Based on the initial evaluation and prior reports^{21,22}, a 48 h incubation resulted in acceptable levels of cell death in the B16-F10 cells. Therefore, 48 h was chosen as the optimum incubation time to investigate the anti-cancer properties of chrysin in subsequent analyses²³. After incubation, the MTT solution (5 mg/mL) was added to the cells and incubated for 4 h at 37 °C. After removing the medium, DMSO was added, and the optical density was determined at 570 nm using an ELISA Reader (BioTek Instruments, Inc. USA). Cell viability was calculated by the following formula: Cell viability (%) = [OD (chrysin-treated) – OD (Blank) / OD (non-treated control) – OD (Blank)] \times 100. Dose-response curves and IC₅₀ values were obtained using the GraphPad Prism software.

Trypan Blue exclusion dye was used to determine the viability of cells exposed to RT alone or combined with chrysin. For this aim, B16-F10 cells were cultivated in T25 flasks (3×10^5 cells). After 24 h of incubation, the cells were treated with different concentrations of chrysin (30, 50, and 70 μ M) for 2 h, then subjected to 2 and 4 Gy (Gy) radiation. Untreated cells were used as controls. The applied RT doses were chosen according to published reports^{24,25}, and studies by this group^{16,26}. The viability of B16-F10 cells was calculated by observation under a phase-contrast microscope after 48 h of incubation (optimum time point obtained by MTT assay). Cell viability was calculated by the following formula: Cell viability (%) = number of viable cells / total cell \times 100. Both experiments were conducted in triplicate, and the results are presented as the mean of three replicates.

Combination therapy condition and analysis

The optimum concentration of chrysanthemum that was acquired by the MTT assay was applied to treat the cells 2 h before RT exposure (2 and 4 Gy). Following 48 h of incubation, the viability of all experimental groups was examined using a Trypan Blue exclusion dye assay. The obtained data were presented as the fraction affected (Fa), ranging from 0 to 1 (Fa = 0 denotes 100% viability and Fa = 1 denotes 0% viability), and analyzed using CompuSyn software V. 7 according to the Chou-Talalay method. The CI values indicate the mode of interaction between chrysanthemum and RT. The CI < 1 represents synergism, CI = 1 represents an additive impact, and CI > 1 illustrates antagonism⁸. To avoid the cytotoxic effect of chrysanthemum at higher concentrations, it was used at concentrations around the IC₅₀ for all experiments. Combination therapy with the selected concentration of chrysanthemum and RT caused maximal anti-cancer effects, as outlined with CI.

Radiation treatment

The cell culture flasks were exposed to a 6 MV photon beam using an Elekta linear accelerator (Elekta Solutions AB, Sweden). The flasks were sandwiched between water-equivalent slab phantoms at the source to surface distance of 100 cm and the field size of 20 × 20 cm². The flasks were located at a depth of 2 cm from the surface, and 5 cm of slab phantom was used under the flasks. A total radiation dose of 4 Gy with a dose rate of 300 cGy/min was delivered to the cells.

Apoptosis determination by flow cytometry analysis

To assess apoptosis induction, 2 × 10⁵ B16-F10 cells were seeded in 60 mm dishes and incubated overnight. B16-F10 cells were exposed to chrysanthemum alone (60 μM), radiation alone (4 Gy), and combination therapy (60 μM of chrysanthemum + 4 Gy radiation with an incubation time of 48 h. In combination therapy, the cells were treated with chrysanthemum for 2 h and then subjected to radiation and incubated for another 48 h. The cells were harvested from all experimental groups, including untreated cells. Flow cytometric analysis was done using an Annexin V/PI apoptosis detection kit (ebioscience, USA; Cat No: 88-8005-72). Harvested cells were washed with phosphate buffer saline (PBS) and resuspended in binding buffer. The cells were stained with binding buffer containing 5 μL FITC-conjugated Annexin V for 15 min at RT. After washing with binding buffer, the cells were stained with 5 μL PI solution. The percentage of apoptotic cells was determined in all experimental groups using a FACSCalibur (BD Bioscience, USA). The obtained data were analyzed using the FlowJo software ver. X.0.7^{27,28}. Three independent experiments were performed.

Western blotting assay in B16-F10 cells exposed to mono-and combination therapy

Western blot analysis assessed PD-L1, STAT3, p-STAT3, and β-actin protein expression. In this pathway, B16-F10 cells (2 × 10⁵) were grown in 60 mm dishes for overnight. In the following, cells were treated with chrysanthemum alone (60 μM), radiation alone (4 Gy), or a combination of them and incubated for 48 h. In combination therapy, the B16-F10 cells were treated with chrysanthemum for 2 h and then exposed to radiation and incubated for another 48 h. At the end of the incubation, the cells were harvested, lysed with RIPA buffer containing PMSF and protease inhibitor, and incubated for 30 min at 4 °C. The homogenates were centrifuged at 13,000×g for 15 min at 4 °C, and the protein concentrations were determined using a BCL kit (Pierce, Rockford, IL, USA). After boiling samples (5 minutes), 50 μg of each protein sample was run on 12% SDS-PAGE to separate proteins²⁹. Next, the separated proteins were transferred onto polyvinylidene fluoride membranes. To avoid nonspecific interactions, membranes were blocked with TBS-T buffer (20 mM Tris-HCl, 137 mM NaCl, and 0.05% v/v Tween 20) containing 5% skim milk and incubated for 60 min at 25 °C. Membranes were incubated with primary antibodies against anti-STAT3 (Cat. no. 678002) and p-STAT3 (Cat. no. 651002), anti-PD-L1 (Cat. no. sc-518027), and anti-β-actin (Cat. no. sc-47778) against the target proteins at 4 °C overnight. Following two washes with TBS-T, the membranes were incubated with TBS-T-containing secondary antibody (Santa Cruz, Cat. no. sc-516102) for 60 min at 25 °C. After washing the membranes, the protein bands were visualized by enhanced chemiluminescence (Roche, UK) using X-ray film. ImageJ 1.6 software was used to calculate each protein band's signal intensity, which was then normalized to the respective β-actin control³⁰⁻³².

Detection of CRT exposure on cancer cell surfaces in B16-F10 cells exposed to mono-and combination therapy

Cells were seeded and treated in the same concentration and procedure as described in the previous parts. All experimental groups were stained with a PE-conjugated CRT monoclonal antibody (Cat. no. ADI SPA 601PE D, Enzo Life Sciences) and evaluated using a FACSCalibur (BD Bioscience, USA). The acquired data were analyzed using FlowJo software ver. X.0.7.

Determination of HSP70, HMGB1, and ATP levels in B16-F10 cells exposed to mono-and combination therapy

B16-F10 cells were seeded and treated with the same manner as described above. Supernatants were collected from all experimental groups (untreated and treated cells) to detect the levels of HSP70, HMGB1 and using a commercially available ELISA kit (HMGB1: MBS722248 and HSP70: MBS722559, MyBioSource, Inc., USA). ATP release was determined using a standard curve generated from standard solutions using an ATP Determination Kit (Thermo Fisher Scientific, Waltham, MA, USA).

Intracellular ROS measurement in B16-F10 cells exposed to mono-and combination therapy

To measure intracellular ROS levels generated by the treatment regimen, we used the fluorescence dye 2',7'-Dichlorodihydrofluorescein diacetate (DCFH-DA) ((Sigma Chemical Co. (St. Louis, MO, USA)) that can penetrate the cells and interact with intracellular ROS and form fluorescent dichlorofluorescence (DCF)³³.

Indeed, DCFH-DA is oxidized by ROS to generate a fluorescent DCF within the cells. In brief, the cells were treated using the same procedure described in the previous part. After 48 h incubation, the cells were trypsinized with 0.25% trypsin and resuspended in 2 ml PBS. Then, 1 ml of cells were incubated with 1 μ l of DCFH-DA (1 mg/ml) and kept for 30 min at 37° under dark conditions. The cells were then washed with serum-free medium or warmed PBS three times to remove the free DCFH-DA. The fluorescence of DCFH-DA was determined using a microplate reader (BioTek Instruments, Inc. USA) with an excitation wavelength of 485 \pm 10 and an emission wavelength of 530 \pm 12.5 nm.

Isolation and differentiation of bone marrow-derived dendritic cells (BMDCs) from murine

DCs were isolated from 7-day bone marrow cultures of C57BL/6 mice based on the previously defined procedure³⁴. In brief, mice were euthanized with an overdose of sodium pentobarbital (> 100 mg/kg) by intraperitoneal injection, followed by cervical dislocation. In the following, femurs were removed and separated from the surrounding tissue. After cleaning the whole bone with 70% ethanol, it was washed with PBS. After cutting both ends of the bone with scissors, an insulin syringe was used to flush bone marrow with PBS. The acquired leukocytes were filtered using a 40 μ m cell strainer to collect the single-cell suspension. Approximately 2×10^7 cells per femur were obtained after one washing step with PBS. The following procedure was performed to prepare mature BM-derived DCs. At day 0, the isolated leukocytes (2×10^6) were cultivated in 100 mm culture dishes containing 10 mL of a 1:1 mixture of conditioned media from B16-F10 cells and DCs media (RPMI-1640 with 10% FBS, penicillin-streptomycin, and L-glutamine) supplemented with 20 ng/mL granulocyte-monocyte colony-stimulating factor (GM-CSF) (PeproTech, Rocky Hill, NJ, USA). An additional 10 mL of DCs complete medium was added at day 3. A fresh culture medium consisting of a 1:1 mixture of DCs complete media and GM-CSF-supplemented conditioned media (20 ng/mL) was replaced with 10 mL of DCs supernatant on day 6. The supernatants from all culture groups were collected at day 7 to detect IL-12 levels. An experimental group of leukocytes grown without conditioned media was used as a negative control. A group of leukocytes treated with 100 ng/mL LPS at day 6 was used as the positive control (supernatant was collected at day 7). Conditioned media was prepared by culturing and treating B16-F10 cancer cells in 60 mm dishes for 48 h according to the defined treatment regimen (mono-and combination therapies). The supernatant was collected, centrifuged, and filtered in the following step to prepare the conditioned media.

ELISA-based assessment of functional maturation of BMDCs

Mature DCs were generated based on the method described in the previous study³⁵. The supernatant from the DCs was collected and analyzed to evaluate IL-12 secretion using a commercially available ELISA kit (mouse IL-12 p70, Cat. No. 88712122; Invitrogen).

Statistical analysis

Each experiment was performed in triplicate, and all data are presented as the mean \pm standard deviation (SD). Data analyses were performed using GraphPad Prism, version 9.01. All results were compared using one-way analysis of variance (ANOVA) followed by a post-hoc test using Tukey's pairwise comparison assay. Statistical significance was set at $p < 0.05$, using GraphPad Prism version 9.01.

Results

Growth inhibitory effects of chrysin alone and in combination with RT in B16-F10 cells

The cytotoxic effect of chrysin on the viability of B16-F10 cells was assessed using an MTT assay. Figure 1a depicts the dose-response curve for the inhibitory effects of chrysin on B16-F10 cells. Based on these findings, the IC50 values of chrysin were $64 \pm 3.67 \mu\text{M}$.

To investigate whether chrysin can intensify the anti-cancer effects of RT on B16-F10 cells, the cells were exposed to different doses of chrysin alone, radiation alone, or combination therapy (the cells treated with chrysin 2 h and then subjected to radiation and incubated for another 48 h). Table 1 depicts the Fa and CI values calculated using Compusyne software for B16-F10 cells exposed to various combinations of chrysin and radiation. Our results showed that combining chrysin and radiation had a synergistic anti-cancer effect on B16-F10 cancer cells.

Figure 1b shows the Fa-CI plot obtained using Compusyn software. According to the Chou-Talalay method, CI values < 1 indicate a synergistic effect. In this work, a combination of 60 μM of chrysin and 4 Gy radiation caused a strong synergistic effect with CI value of 0.66. As shown in Fig. 1c, the cell viability of the irradiated group reduced from $74.61 \pm 5.38\%$ to $59.67 \pm 3.67\%$ in chrysin-treated cells to $35.55 \pm 6.7\%$ in the cells exposed to combinational therapy with chrysin (60 μM) and radiation (4 Gy). Combining chrysin (60 μM) and radiation (4 Gy) remarkably reduced cell viability compared to each monotherapy treatment. In further experiments, the cells were treated with 60 μM of chrysin for 2 h and then subjected to 4 Gy irradiation as the optimum combination therapy.

Apoptosis induction in the B16-F10 cells exposed to chrysin and /or RT

It is well established that ICD is a type of apoptosis that stimulates a specific anti-cancer immune response³⁵. Accordingly, we proposed to examine whether chrysin alone as monotherapy or in combination with radiation can cause apoptosis in B16-F10 cells. Flow cytometric analysis was conducted 48 h after monotherapy and combination therapy using the Annexin V/PI double staining assay. Figure 2 shows that chrysin alone and in combination with radiation could induce apoptosis in B16-F10 cells. Apoptosis in B16-F10 cells treated with chrysin alone (60 μM) was $48.23 \pm 6.3\%$. The cells subjected to radiation (4 Gy) exhibited 31.5 ± 5.3 apoptosis. Interestingly, the combination therapy led to a remarkable apoptotic percentage of $81.45 \pm 3.1\%$. These findings

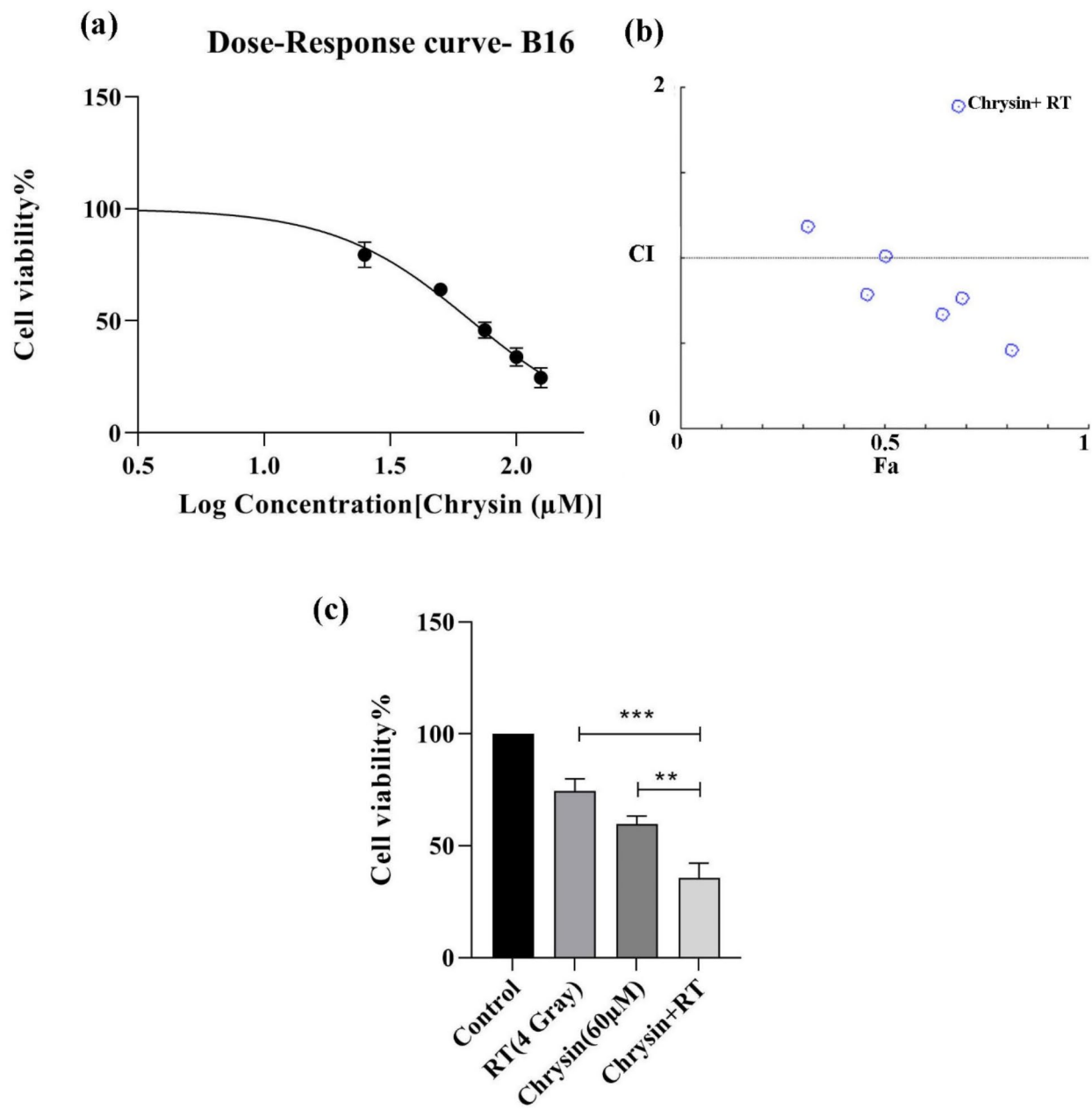


Fig. 1. (a) Dose-response curve of chrysin created using GraphPad Prism software and data obtained by MTT assay in B16-F10 cells. (b) A Fa-CI plot for different combinations of RT and chrysin was obtained using Trypan blue data and Compusyn software. (c) Viability of B16-F10 cancer cells treated with monotherapy and the optimum synergistic combination therapy of RT and chrysin.

indicate that combining chrysin and radiation significantly enhances cell death through apoptosis-mediated pathways, compared to monotherapy with either chrysin or radiation.

An assessment of CRT expression in the surface of B16-F10 cells subjected to chrysin and/or RT

As defined in the previous part, CRT surface exposure on cancer cells is an important marker of ICD induction that triggers the uptake of dying tumor cells by DCs. In this study, surface exposure of CRT was examined in all experimental groups after 48 h to determine the possible effect of chrysin as an inducer and/or enhancer of ICD induced by radiation. As depicted in Fig. 3, CRT expression was detected $4.5 \pm 3\%$ in the non-treated group, $32.13 \pm 3.14\%$ in cells treated with chrysin alone ($60 \mu\text{M}$), and $24.45 \pm 5.2\%$ in the cells exposed to radiation alone (4 Gy). A significant increase was observed in the CRT expression ($60.34 \pm 4.5\%$) in the cells exposed to chrysin ($60 \mu\text{M}$) in combination with RT (4 Gy) as compared with monotherapy-treated groups.

Dose chrysin	Radiotherapy	Fa	CI
30.0	2.0	0.313	1.18679
60.0	2.0	0.506	1.01099
90.0	2.0	0.693	0.76665
30.0	4.0	0.459	0.78428
60.0	4.0	0.644	0.66683
90.0	4.0	0.815	0.45725

Table 1. Fraction of affected cells (Fa) and combination index (CI) for different combinations.

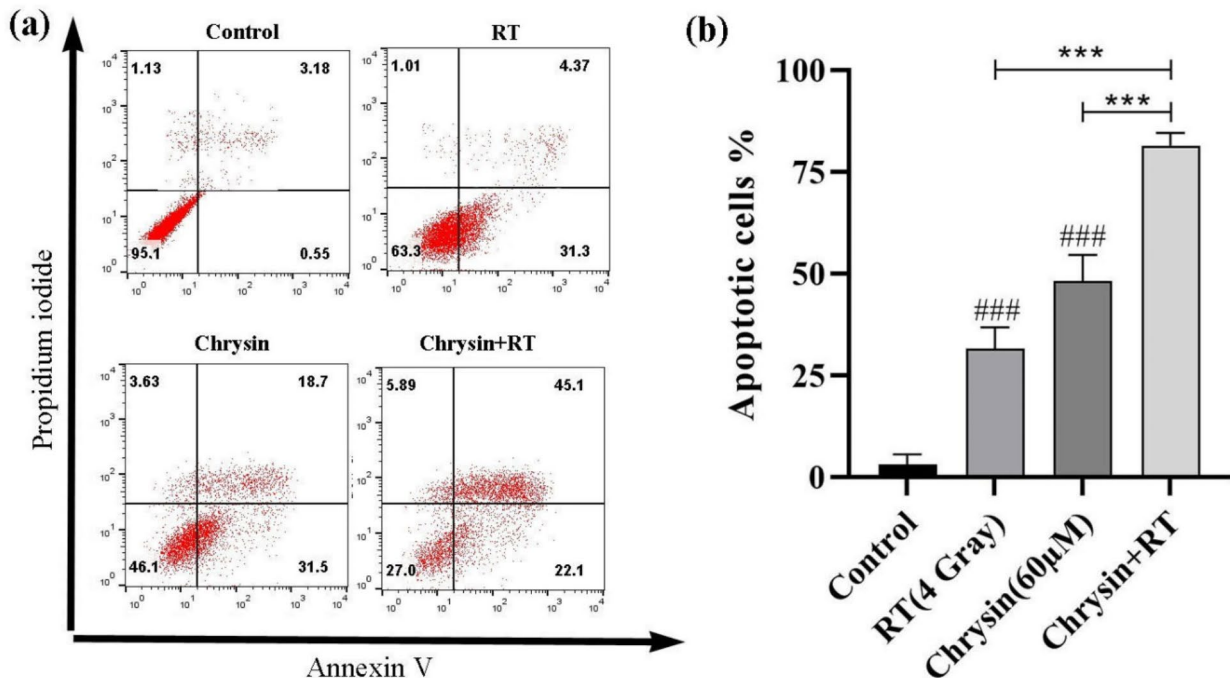


Fig. 2. Determination of Apoptosis by Annexin V/PI double staining assay. (a) Representative dot plot and (b) Graph bar of apoptotic B16-F10 cells treated with radiotherapy (RT), chrysin and chrysin + RT. The assay was conducted in three independent experiments and data were shown as mean \pm SD. ### $p < 0.001$ compared with the control group. *** $p < 0.001$ compared with each treatment group.

Evaluation of HMGB1 secreted by B16-F10 cells exposed to chrysin and/or RT

The nuclear molecule called HMGB1 is secreted by cancer cells during the ICD. It was found that HMGB1 can induce T-cell-mediated immune responses against tumors³. To assess ICD induction, the secretion level of HMGB1 was examined in the supernatants of B16-F10 cells exposed to chrysin alone or in combination with radiation. Based on the obtained results, HMGB1 level increased from 5.05 ± 0.4 ng/mL in the non-treated group (control) to 10.7 ± 0.5 ng/mL ($p < 0.001$) and 8.1 ± 0.2 ng/mL ($p < 0.001$) ng/mL in the chrysin and radiation groups, respectively (Fig. 4a). The level of HMGB1 secretion in the B16-F10 exposed to combinational therapy was significantly higher (13.56 ± 0.05 ng/mL) than that in monotherapies, chrysin, and radiation ($p < 0.001$).

Evaluation of HSP70 secreted by B16-F10 cells exposed to chrysin and/or RT

It has been demonstrated that immunogenic death of cancer cells usually releases heat shock protein 70 (HSP70) into the extracellular environment due to ER stress⁴. Therefore, we investigated the secretion level of HSP70 protein in B16-F10 cells treated with chrysin and/or radiation. As we observed with HMGB1 release, in a similar pattern shown in Fig. 4b, monotherapy-treated B16-F10 cells had higher levels of HSP70 than non-treated control groups (chrysin: 11.7 ± 1.04 , ($p < 0.001$) and radiation: 6.1 ± 0.2 ($p < 0.001$)). The combinational treatment with chrysin and radiation caused a significant rise in the secretion level of HSP70 (19.2 ± 0.47 ng/mL) as compared with cells exposed to individual therapy ($p < 0.001$).

Evaluation of ATP levels by B16-F10 cells exposed to chrysin and/or RT

ATP is another immunogenic signal secreted by dying tumor cells during autophagic stress. ATP mediates the attraction of macrophages and DCs into the tumor sites by purinergic⁵. In other words, beyond CRT expression and the release of HSP70 and HMGB1, ATP release by dying cells is one of the hallmarks of ICD. To explore

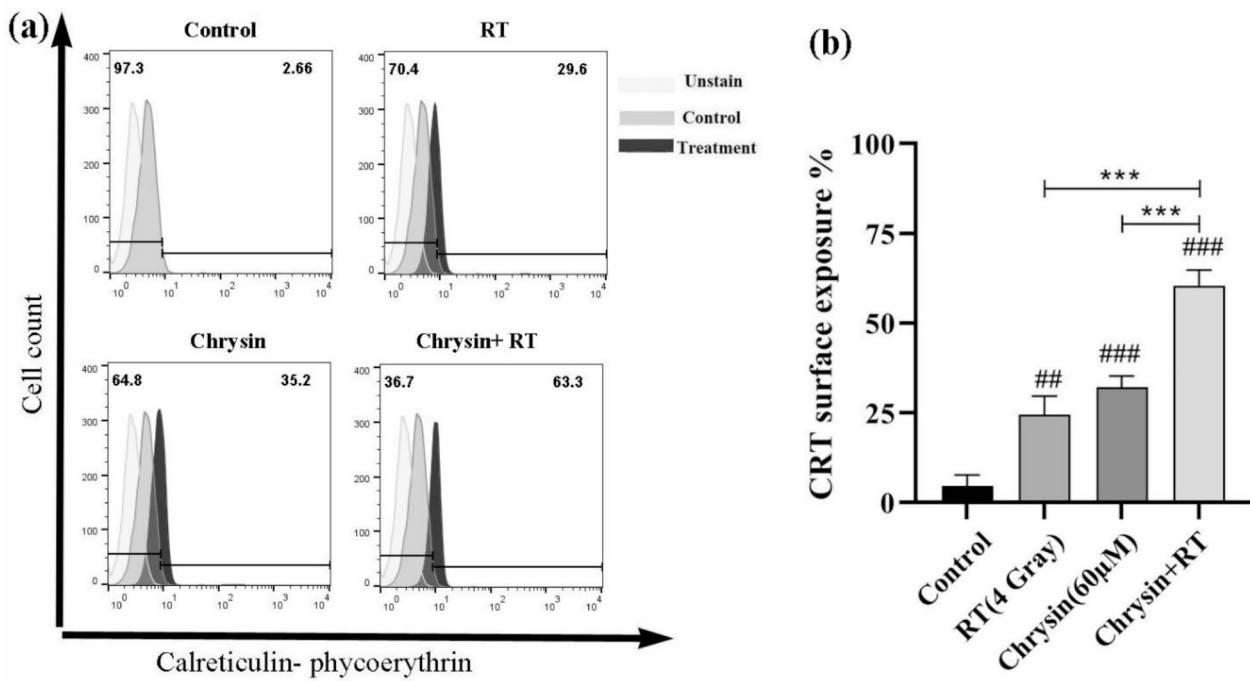


Fig. 3. Flow cytometry of calreticulin (CRT) surface exposure by monoclonal phycoerythrin-conjugated CRT antibody. **(a)** Representative histogram and **(b)** graph bar of CRT surface exposure in B16-F10 cells treated with radiotherapy (RT), chrysin, and chrysin + RT. The assay was conducted in three independent experiments, and data are shown as the mean \pm SD. ##p < 0.01 and ###p < 0.001 compared with the control group. ***p < 0.001 compared with each treatment group.

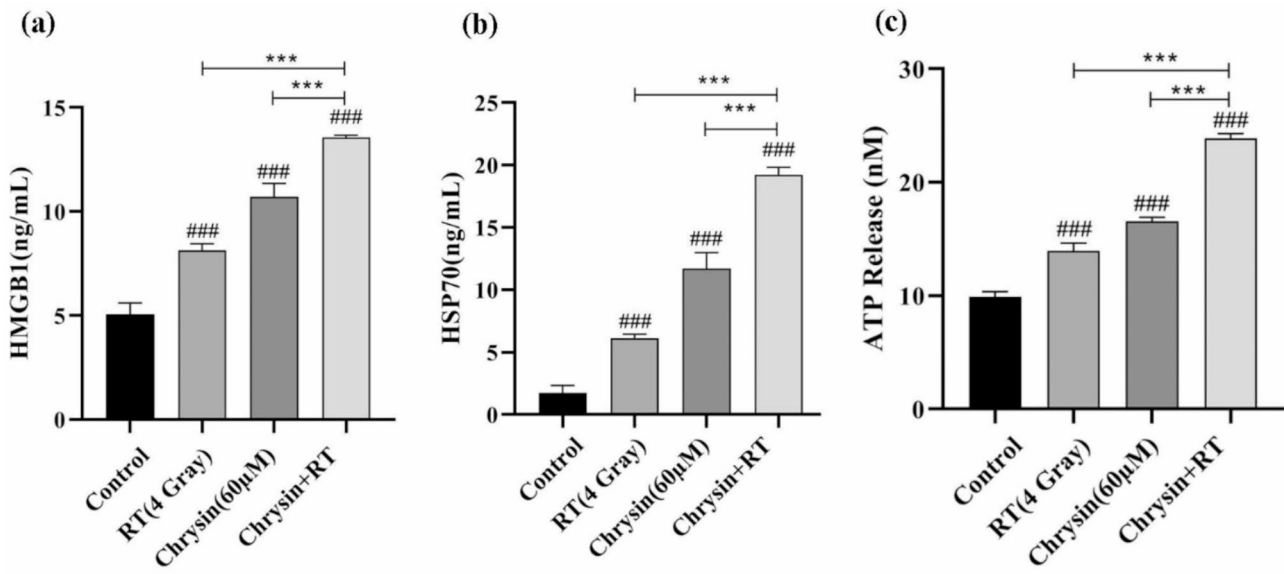


Fig. 4. Detection of **(a)** HMGB1, **(b)** HSP70, and **(c)** ATP release in the supernatants of B16-F10 cells exposed to radiotherapy (RT), chrysin, and chrysin + RT. HMGB1 and HSP70 levels were measured using an ELISA Kit. ATP levels of ATP is determined using an ATP Determination Kit. All experiments were repeated three times, and data were shown as mean \pm SD. ###p < 0.001 compared with the control group. ***p < 0.001 compared with each treatment group.

the potential effect of mono- and combinational therapies in inducing ICD, we determined ATP secretion in all experimental groups. The ATP levels in the supernatants were considerably higher in the chrysin and radiation groups than in the untreated control group (Fig. 4c). (chrysin: 16.54 ± 0.29 , $p < 0.001$ and 13.9 ± 0.56 radiation $p < 0.001$). The combination of chrysin and radiation significantly increased the secretion of ATP compared to that in cells exposed to individual therapy ($p < 0.001$). These data suggested that monotherapy and combination treatment can promote the expression of ICD biomarkers in B16-F10 cells (Fig. 4).

The effect of chrysin alone and in combination with RT on p-STAT3 and PD-L1 levels

Previous studies have demonstrated that chrysin inhibits STAT3 expression, which is constitutively active in most human cancers and has an essential role in cancer development. The phosphorylated/active form is p-STAT3, which contributes to the growth/survival of cancer cells, resistance to chemotherapeutics, and immunosuppressive status in the tumor niche³⁵. Previous studies have revealed that chrysin can suppress STAT3 activity and sensitize cancer cells to chemotherapeutic drugs. We sought to determine whether chrysin could suppress p-STAT3 in B16-F10 cell lines harboring constitutively active STAT3. After 48 h of treatment with monotherapies (chrysin or radiation) and combination treatment, the cells were subjected to evaluation of p-STAT3 by immunoblotting. As depicted in Fig. 5a and c (Sup. 5), treatment of B16-F10 cells with chrysin monotherapy decreased the level of p-STAT3 compared to the untreated group (control). Notably, the level of p-STAT3 was remarkably decreased in the cells exposed to combinational treatment compared to the single chrysin-treated cancer cells ($p < 0.05$).

Evidence shows that PDL-1 is a strong immune inhibitor in most human tumors, causing immune evasion by the tumor cells⁹. In better words, PD-L1 has an immunosuppressive function in tumor development. Accordingly, we analyzed the levels of PD-L1 following mono- and combinational treatment in B16-F10 cells after 48 h. As shown in Fig. 5a and b, there was a significant decrease ($p < 0.001$) in the level of PDL1 in cells treated with chrysin compared to the untreated group. However, a single treatment of B16-F10 cells with RT (4 Gy) did not significantly change PDL-1 expression levels. PDL-1 expression was shown by a remarkable decline in cells exposed to combination treatment compared to those exposed to radiation ($p < 0.001$) and chrysin ($p < 0.01$). These findings support the ability of chrysin to enhance the efficacy of radiation.

Combination of chrysin and RT intensifies ROS generation

ROS plays an essential role in inducing apoptosis³⁶. The regulation of ROS formation was assessed in the cells exposed to the chrysin and irradiation alone and their combination. The intracellular content of ROS was determined by a fluorescence-sensitive dye (DCF-DA) that detects various forms of ROS. As depicted in Fig. 6, the level of ROS was elevated in the cells treated with single therapy of RT ($p < 0.01$) and chrysin ($p < 0.001$). As expected, ROS production was substantially increased in the cells similarly exposed to combination therapy.

IL-12 production in BM-DCs exposed to the conditioned media from B16-F10 cells

As evidenced, functional maturation of DCs is correlated with high expression of pro-inflammatory cytokines such as IL-12³⁷. In addition, IL-12 secretion can elicit a T cell-mediated immune response by DCs against

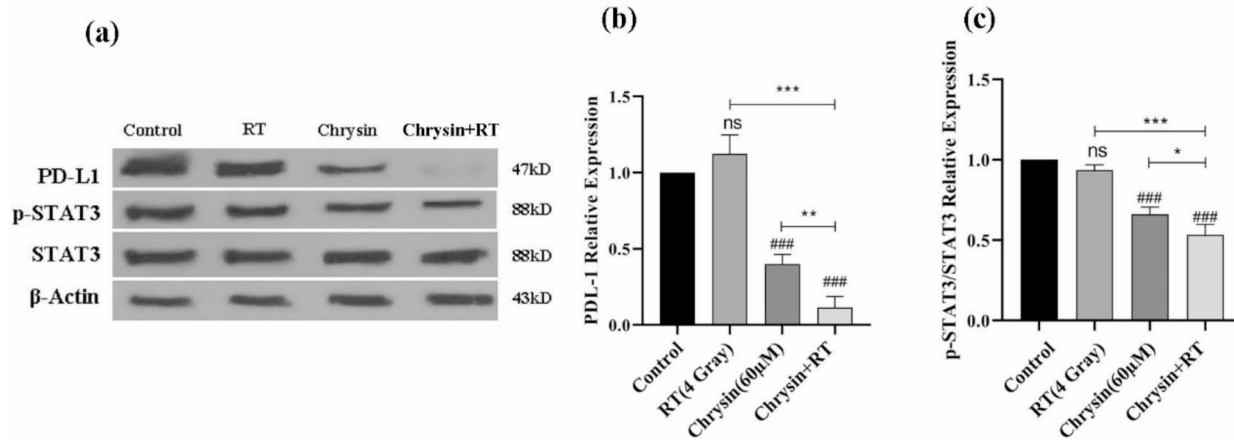


Fig. 5. Western blot analysis of p-STAT3 and PDL1 expression in B16-F10 cells exposed to radiotherapy (RT), chrysin, and chrysin + RT. (a) Representative analysis, (b) PDL1 relative expression, and (c), p-STAT3 /STAT3 relative expression. All experiments were repeated three times, and data were shown as mean \pm SD. $### p < 0.001$ compared with the control group. $*p < 0.05$, $** p < 0.01$ and $*** p < 0.001$ compared with each treatment group. ns; non-significant. The uncropped version of western blotting analysis was presented in Sup. 5.

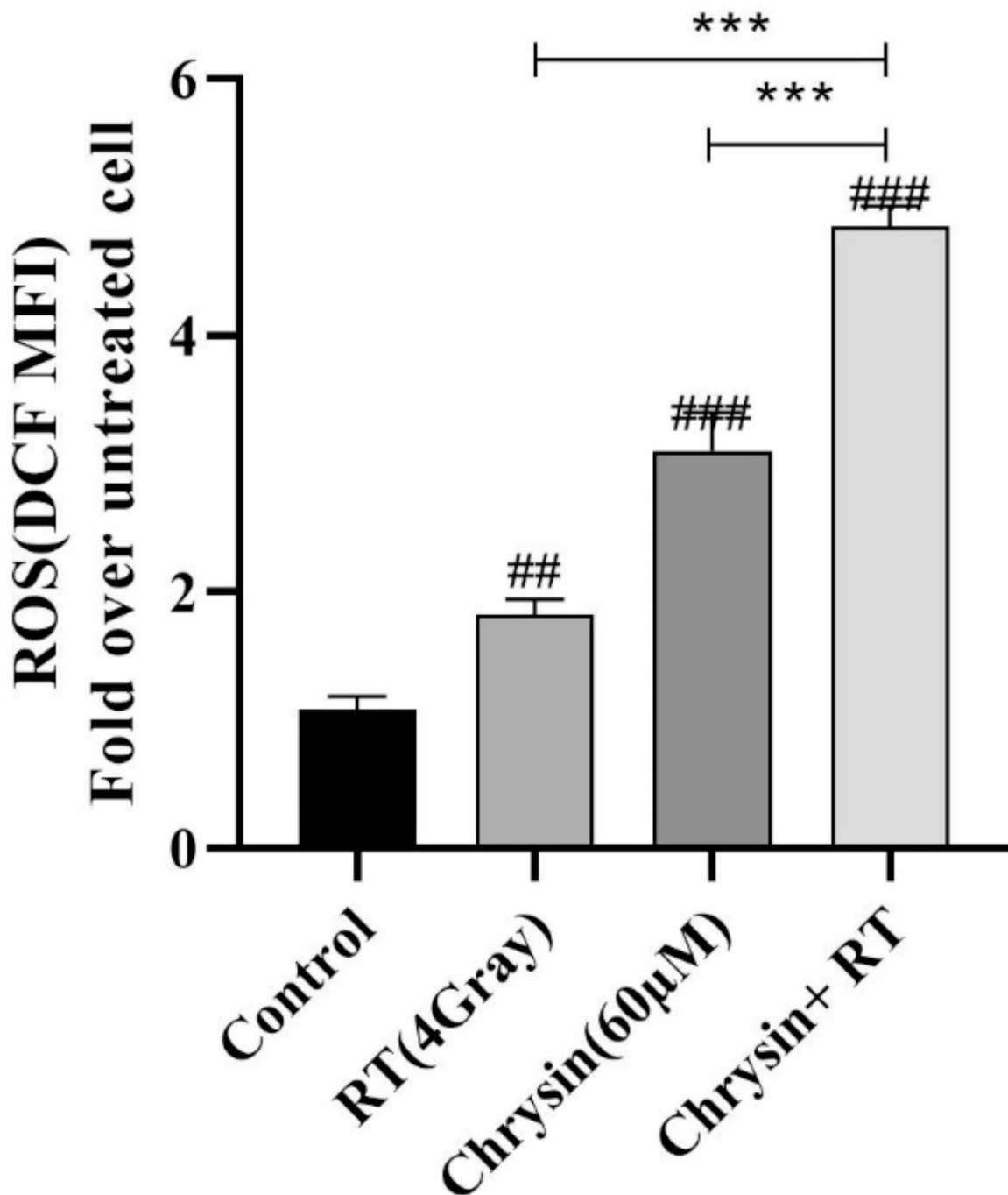


Fig. 6. Detection of ROS production in the cells exposed to RT, chrysin, and chrysin + RT. ROS levels were measured by a microplate reader using the ROS-sensitive dye (DCF-DA) in B16-F10 cells. All experiments were repeated three times, and data were presented as mean \pm SD. ## $p < 0.01$ and ### $p < 0.001$ compared with the control group. *** $p < 0.001$ compared with each treatment group.

cancer cells. To examine the effect of chrysin alone or in combination on the functional maturation of DCs and activation of activated T cell-mediated responses, we measured IL-12 levels in the supernatants of DCs upon exposure to the conditioned media of B16-F10 cells. Based on the data obtained by ELISA, IL-12 levels significantly increased in BM-DCs exposed to the conditioned media from B16-F10 cells exposed to chrysin alone ($p < 0.001$) compared to that observed in BM-DCs treated with conditioned media from the untreated

group (control) (Fig. 7). Interestingly, the level of IL-12 significantly went up from 35.7 ± 2.5 and 47.3 ± 1.1 pg/mL in the supernatant of DCs respectively exposed to condition media of radiation and chrysin-treated B16-F10 cells to 75.3 ± 3.5 pg/mL in the group received chrysin and radiation as the combinational treatment ($p < 0.001$).

Discussion

Immunotherapy is one of the promising approaches in the treatment of various types of cancer. Cancer immunotherapy acts by activating patients' immune response against tumor cells. Cancer-mediated immunosuppression is a major challenge that causes treatment failure in cancer immunotherapy³⁸.

ICD induction is a promising modality for the induction of specific anti-tumor immune responses and reversal of immune suppression in cancer immunotherapy. Several types of chemotherapeutic, natural agents, and RT are known as ICD inducer. Beyond the direct effect of RT on dsDNA, RT can also elicit an immunogenic variant of regulated cell death and activate tumor-targeting immune responses⁹. RT also exerts indirect damage by forming ROS³⁹. IR-induced immune response against tumor cells is mediated by a series of events, one of which is the ICD induction⁴⁰. RT often employs high-energy radiation to ionize atoms/molecules for damaging dsDNA and inducing ICD in cancer cells. High dosage of RT causes harmful impacts on the normal surrounding tissue; hence, delivering a controlled dose of radiation is an important option in cancer therapy.

Over the past few years, considerable interest has been paid to identify natural compounds with the ability to induce or enhance anti-cancer immunity⁸. Chrysin is a natural flavonoid compound that exerts beneficial anti-cancer effects through different mechanisms. Previous studies have demonstrated that chrysin causes apoptotic cell death through ER Stress and ROS production in tumor cells¹³. Different studies have shown that chrysin inhibits the activation of STAT3, suggesting its potential as a candidate for the induction and /or enhancement of ICD⁴¹. Our previous study also demonstrated that chrysin exhibits a synergistic anti-cancer effect with RT and may act as a radiosensitizer in breast cancer cell line¹⁶. Therefore, we hypothesized that chrysin could enhance the RT-induced ICD in B16-F10 cells, a mouse model of melanoma with hyperactive STAT3. In addition, we investigated whether chrysin could induce ICD as a natural agent.

This study observed a synergistic anti-tumor effect from the combined treatment of chrysin and RT, likely due to the different mechanisms of chrysin and RT against cancer therapy. Several studies have revealed that chrysin can induce ROS production⁴², and this effect can potentiate RT-induced ROS generation. On the other hand, it has been shown that chrysin can sensitize cancer cells to different chemotherapeutic agents and reduce

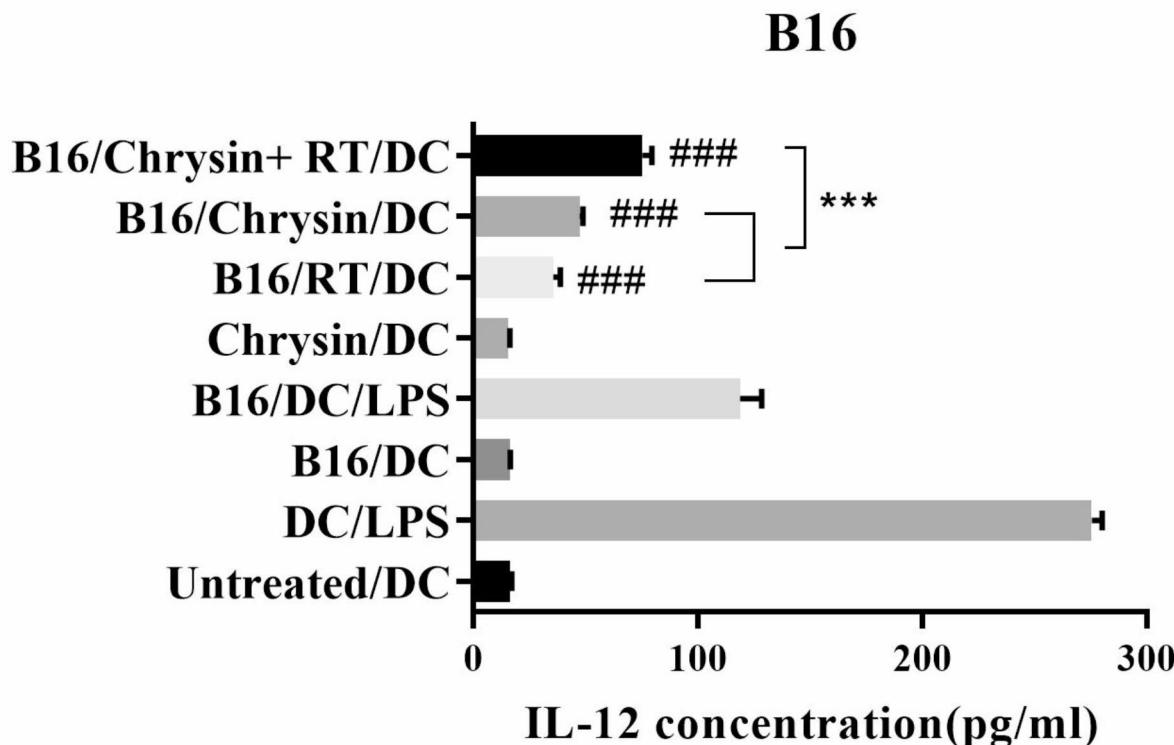


Fig. 7. IL-12 secretion by DCs exposed to conditioned media of B16-F10 cells treated with radiotherapy (RT), chrysin and chrysin + RT. IL-12 secretion was detected by ELISA Kit and data are presented as mean \pm SD. All experiments were repeated three times. *** $p < 0.001$ compared with the untreated group (control). ** $p < 0.001$ compared with each treatment group.

their resistance to treatment through different mechanisms, such as induction of apoptosis and inhibition of STAT3 expression^{13,43}.

The induction of apoptosis is a fundamental strategy in cancer treatment, and multiple signaling pathways are involved in this type of death. Several studies have demonstrated that chrysin prevents proliferation and induces apoptosis in most cancer cells³. Our results showed that chrysin induced apoptosis in the B16-F10 cells. The combination of chrysin with RT augmented the percentage of apoptotic cell population. These findings imply that combination therapy can potentiate the radiation sensitivity of B16-F10 cells by increasing the number of apoptotic cells. Apoptosis is the appropriate type of death for cancer cells and induction of ICD leads cancer cells to go through the apoptosis and expose or release DAMPs factors¹².

Cell surface exposure of CRT and secretion of HMGB1, HSP-70, and ATP are common biomarkers for predicting the capacity of applied interventions to induce ICD. The largest fraction of CRT is located in the lumen of the ER, which is exposed to the outer surface of the plasma membrane during ER-stress and pre-apoptotic events. Cells that expose CRT on their surface can be efficiently engulfed by DCs⁴⁴. Previous studies have demonstrated that RT can induce CRT expression in different cancer cells in vivo and in vitro^{45,46}. It has been demonstrated that RT can induce CRT expression in different cancer cells in vivo and in vitro⁴⁷. In the current study, flow cytometry results revealed a substantial increase in CRT expression in B16-F10 cells after exposure to chrysin and RT alone, and more importantly, combination treatment significantly stimulated CRT expression.

The release of HMGB1 can activate general autophagy and mitochondria-related autophagy⁴⁸. Besides, HMGB1 and HSP70 are able to induce DCs through binding to TLR4 receptor and prime Th1 response against tumor cells. Extracellular released ATP from dying cells provides recruitment signals for monocytes, macrophages, and DCs⁴⁹. Several lines of studies have confirmed that HMGB1, HSPs and ATP are the most important DAMPs produced following RT in cancer cells such as melanoma⁵⁰. Our results from the irradiation of B16-F10 cells were in line with those reported in previous studies^{51,52}. In addition, we observed a significant increase in HMGB1, HSP-70, and ATP levels in B16-F10 cells after exposure to chrysin alone. These findings indicate that B16-F10 cells may release these biomarkers into the extracellular, which leads to further immune cell recruitment to their proximity. Thus, chrysin and radiation as individual treatments can be used as ICD inducers in B16-F10 cells. Interestingly, the combination treatment of B16-F10 cells with chrysin and RT resulted in significantly higher levels of CRT, HMGB1, HSP70, and ATP compared to B16-F10 cells exposed to each agent alone. This finding may be related to the suppressive role of chrysin on STAT3 activation in B16-F10 cells that harbor constitutively active STAT3¹³. Consistently, previous reports have shown that suppression of STAT3 in cancer cell lines with hyperactive STAT3 can enhance the ability of ICD-inducers in eliciting DAMP release^{35,53}.

In this study, the anti-tumor immune response mechanism of chrysin was explored in B16-F10 cells in association with STAT3 and PD-L1 signaling. STAT3 and PD-L1 play various biological roles in cancer progression, metastasis, and modulation of the immune microenvironment in cancer cells⁵⁴. STAT3 signaling plays a substantial role in immune escape and modulating the crosstalk between tumor cells and the immune cells⁵⁵. The latter is mediated by crosstalk between immune cells and tumor cells such as CD8+ T-cells, Tregs, and NK cells⁵⁶. It has also been reported that STAT3 triggers immunosuppression through upregulating PD-L1. Accumulating evidence indicated that STAT3 binding to the PD-L1 promoter can drives PD-L1 transcription, thereby triggering immunosuppression and enabling cancer cells to evade immune surveillance⁵⁷. Overexpression of PD-L1 is significantly associated with the phosphorylated form of STAT3 in many types of cancers⁵⁸. We found that chrysin-mediated suppression of STAT3 phosphorylation and downregulated PD-L1 expression, indicating the close interaction between STAT3 and PD-L1. Interestingly, the suppression was intensified by the combination of chrysin and radiation, demonstrating the success of the combination therapy. However, RT alone did not cause a significant change in PDL-1 and p-STAT3/ STAT3 expression levels compared with the control group. In line with the results found for PDL-1, prior studies have reported that RT simultaneously stimulates ICD and increases PD-L1 expression in cancer or immune cells. This suggesting that combination therapy could be a promising strategy to overcome the immunosuppressive effect of RT⁵⁹.

Finally, we evaluated whether conditioned media from cancer cells treated with chrysin and/or radiation, either as a single agent or in combination, has the potential to mature DCs and trigger Th1-type immune responses. Previous studies have reported that extracellular release of HSP70 and HMGB1 stimulates DCs functional maturation by binding to TLR4, inducing Th1 anti-cancer immune response⁶⁰. We found that incubation of DCs with conditioned media from B16-F10 cells treated with chrysin and/or radiation significantly induced IL-12 secretion compared to the control group. IL-12 secretion is an important marker of DCs activation, reflecting the ability of DCs in eliciting Th1-mediated immune responses. In other words, IL-12 secretion by DCs indicates functional maturation of DC and cell-mediated immunity⁶¹. Combinatorial treatment showed synergistic effects on IL-12 secretion compared to monotherapies and the control groups. These results imply that CRT exposure and HMGB1, HSP70, and ATP secretion by cancer cells exposed to either mono- or combinational treatment could promote functional maturation of DCs and potentially induce Th1 immune response.

Conclusion

In conclusion, chrysin synergistically potentiated the anti-cancer effect of RT in B16-F10 cells with hyperactive STAT3 by inducing ICD and elevating the levels of DAMPs molecules, such as CRT, HMGB1, HSP70, and ATP.

Conditioned media from B16-F10 cells exposed to chrysin alone or in combination with radiation remarkably induced IL-12 secretion in DCs, highlighting the potency of mono- and combination therapy in priming the anti-cancer immune response. Chrysin not only potentiated the anti-cancer effect of radiation but also increased RT-mediated immunogenicity. Further studies are required to examine the molecular pathways by which chrysin induces ICD and how it improves RT-mediated immune responses.

Data availability

The data are available from the corresponding author on reasonable request.

Received: 8 November 2023; Accepted: 10 September 2024

Published online: 05 October 2024

References

1. Sambi, M., Bagheri, L. & Szewczuk, M. R. Current challenges in cancer immunotherapy: Multimodal approaches to improve efficacy and patient response rates. *J. Oncol.* **2019** (2019).
2. Tesniere, A. et al. Molecular characteristics of immunogenic cancer cell death. *Cell. Death Differ.* **15**, 3–12 (2008).
3. Ahmed, A. & Tait, S. W. Targeting immunogenic cell death in cancer. *Mol. Oncol.* **14**, 2994–3006 (2020).
4. Garg, A. D. et al. Molecular and translational classifications of DAMPs in immunogenic cell DEATH. *Front. Immunol.* **6**, 588 (2015).
5. Fucikova, J., Spisek, R., Kroemer, G. & Galluzzi, L. Calreticulin and cancer. *Cell Res.* **31**, 5–16 (2021).
6. Dudek, A. M., Garg, A. D., Krysko, D. V., De Ruysscher, D. & Agostinis, P. Inducers of immunogenic cancer cell death. *Cytokine Growth Factor Rev.* **24**, 319–333 (2013).
7. Hayashi, K. et al. Tipping the immunostimulatory and inhibitory DAMP balance to harness immunogenic cell death. *Nat. Commun.* **11**, 6299 (2020).
8. Jafari, S., Heydarian, S., Lai, R., Aghdam, E. M. & Molavi, O. Silibinin induces immunogenic cell death in cancer cells and enhances the induced immunogenicity by chemotherapy. *BIOIMPACTS* (2022).
9. Jafari, S. et al. Clinical application of immune checkpoints in targeted immunotherapy of prostate cancer. *Cell. Mol. Life Sci.* **77**, 3693–3710 (2020).
10. Wang, J., Wang, H. & Qian, H. -l. Biological effects of radiation on cancer cells. *Military Med. Res.* **5**, 1–10 (2018).
11. Herrera, F. G., Bourhis, J. & Coukos, G. Radiotherapy combination opportunities leveraging immunity for the next oncology practice. *Cancer J. Clin.* **67**, 65–85 (2017).
12. Amiri, M., Molavi, O., Sabetkam, S., Jafari, S. & Montazersaheb, S. Stimulators of immunogenic cell death for cancer therapy: Focusing on natural compounds. *Cancer Cell Int.* **23**, 200 (2023).
13. Moghadam, E. R. et al. Broad-spectrum preclinical antitumor activity of chrysanthemic acid: Current trends and future perspectives. *Biomolecules.* **10**, 1374 (2020).
14. Dabiri, S., Jafari, S. & Molavi, O. Advances in nanocarrier-mediated delivery of chrysanthemic acid: Enhancing solubility, bioavailability, and anticancer efficacy. *BioImpacts*, - (2024).
15. Talebi, M. et al. Emerging cellular and molecular mechanisms underlying anticancer indications of chrysanthemic acid. *Cancer Cell Int.* **21**, 1–20 (2021).
16. Jafari, S. et al. Synergistic effect of chrysanthemic acid and radiotherapy against triple-negative breast cancer (TNBC) cell lines. *Clin. Transl. Oncol.* **25**, 2559–2568 (2023).
17. Zou, S. et al. Targeting STAT3 in cancer immunotherapy. *Mol. Cancer.* **19**, 1–19 (2020).
18. Sun, C., Mezzadra, R. & Schumacher, T. N. Regulation and function of the PD-L1 checkpoint. *Immunity.* **48**, 434–452 (2018).
19. Wang, X. et al. Tumor cell-intrinsic PD-1 receptor is a tumor suppressor and mediates resistance to PD-1 blockade therapy. *Proc. Natl. Acad. Sci.* **117**, 6640–6650 (2020).
20. Galvao, J. et al. Unexpected low-dose toxicity of the universal solvent DMSO. *FASEB J.* **28**, 1317–1330 (2014).
21. Pichichero, E., Cicconi, R., Mattei, M., Muzi, M. G. & Canini, A. Acacia honey and chrysanthemic acid reduce proliferation of melanoma cells through alterations in cell cycle progression. *Int. J. Oncol.* **37**, 973–981 (2010).
22. Xue, C. et al. Chrysanthemic acid induces cell apoptosis in human uveal melanoma cells via intrinsic apoptosis. *Oncol. Lett.* **12**, 4813–4820 (2016).
23. Molavi, O., Torkzaban, F., Jafari, S., Asnaashari, S. & Asgharian, P. Chemical compositions and anti-proliferative activity of the aerial parts and rhizomes of squirting cucumber, Cucurbitaceae. *Jundishapur J. Nat. Pharm. Prod.* **15** (2020).
24. Zoi, V. et al. Curcumin and radiotherapy exert synergistic anti-glioma effect in vitro. *Biomedicines.* **9**, 1562 (2021).
25. Chendil, D., Ranga, R. S., Meigooni, D., Sathishkumar, S. & Ahmed, M. M. Curcumin confers radiosensitizing effect in prostate cancer cell line PC-3. *Oncogene.* **23**, 1599–1607 (2004).
26. Montazersaheb, S. et al. The synergistic effects of betanin and radiotherapy in a prostate cancer cell line: An in vitro study. *Mol. Biol. Rep.* **50**, 9307–9314 (2023).
27. Farjam, A., Siabi-Shabdad, M., Akbarzadehkhaleh, P., Roshanzamir, K. & Molavi, O. Evaluation of the physicochemical and biological stability of cetuximab under various stress condition. *J. Pharm. Pharm. Sci.* **22**, 171–190 (2019).
28. Montazersaheb, S. et al. Targeting TdT gene expression in Molt-4 cells by PNA-octaarginine conjugates. *Int. J. Biol. Macromol.* **164**, 4583–4590 (2020).
29. Rahimi, M. et al. Renoprotective effects of prazosin on ischemia-reperfusion injury in rats. *Hum. Exp. Toxicol.* **40**, 1263–1273 (2021).
30. Farahzadi, R., Fathi, E., Mesbah-Namin, S. A. & Vietor, I. Granulocyte differentiation of rat bone marrow resident C-kit+hematopoietic stem cells induced by mesenchymal stem cells could be considered as new option in cell-based therapy. *Regener. Ther.* **23**, 94–101 (2023).
31. Heidari, H. R. et al. Mesenchymal stem cells cause telomere length reduction of molt-4 cells via caspase-3, BAD and P53 apoptotic pathway. *Int. J. Mol. Cell. Med.* **10**, 113 (2021).
32. Fathi, E., Azarbad, S., Farahzadi, R., Javanmardi, S. & Vietor, I. Effect of rat bone marrow derived-mesenchymal stem cells on granulocyte differentiation of mononuclear cells as preclinical agent in cellbased therapy. *Curr. Gene Ther.* **22**, 152–161 (2022).
33. Xu, H. et al. Deguelin induces the apoptosis of lung cancer cells through regulating a ROS driven Akt pathway. *Cancer Cell Int.* **15**, 1–9 (2015).
34. Garg, S. M., Vakili, M. R., Molavi, O. & Lavasanifar, A. Self-associating poly (ethylene oxide)-block-poly (α-carboxyl-ε-caprolactone) drug conjugates for the delivery of STAT3 inhibitor JSI-124: Potential application in cancer immunotherapy. *Mol. Pharm.* **14**, 2570–2584 (2017).
35. Jafari, S. et al. STAT3 inhibitory statictatin enhances immunogenic cell death induced by chemotherapy in cancer cells. *DARU J. Pharm. Sci.* **28**, 159–169 (2020).
36. Circu, M. L. & Aw, T. Y. Reactive oxygen species, cellular redox systems, and apoptosis. *Free Radic. Biol. Med.* **48**, 749–762 (2010).
37. Wojno, E. D. T., Hunter, C. A. & Stumhofer, J. S. The immunobiology of the interleukin-12 family: Room for discovery. *Immunity.* **50**, 851–870 (2019).
38. Showalter, A. et al. Cytokines in immunogenic cell death: Applications for cancer immunotherapy. *Cytokine.* **97**, 123–132 (2017).
39. Welsh, J. et al. Abscopal effect following radiation therapy in cancer patients: A new look from the immunological point of view. *J. Biomedical Phys. Eng.* **10**, 537 (2020).
40. Sharabi, A. B., Lim, M., DeWeese, T. L. & Drake, C. G. Radiation and checkpoint blockade immunotherapy: Radiosensitisation and potential mechanisms of synergy. *Lancet Oncol.* **16**, e498–e509 (2015).

41. Oliyapour, Y. et al. Chrysin and chrysin-loaded nanocarriers induced immunogenic cell death on B16 melanoma cells. *Med. Oncol.* **40**, 278 (2023).
42. Mani, R., Natesan, V. & Chrysin sources, beneficial pharmacological activities, and molecular mechanism of action. *Phytochemistry.* **145**, 187–196 (2018).
43. Kasala, E. R., Bodduluru, L. N., Barua, C. C. & Gogoi, R. Chrysin and its emerging role in cancer drug resistance. *Chemico-Biol. Interact.* **236**, 7–8 (2015).
44. Fucikova, J. et al. Detection of immunogenic cell death and its relevance for cancer therapy. *Cell Death Dis.* **11**, 1–13 (2020).
45. Okada, K. et al. Calreticulin Upregulation in Cervical cancer Tissues from Patients Following 10 gy Radiotherapy. *Adv. Radiation Oncol.*, 101159 (2022).
46. Huang, Y., Kong, L. & Lu, J. Ecto-calreticulin expression after particle irradiation versus conventional photon irradiation in human cancer cell lines. *Int. J. Radiat. Oncol. Biol. Phys.* **105**, E643 (2019).
47. Okada, K. et al. Calreticulin Upregulation in cervical cancer tissues from patients after 10 gy radiation therapy. *Adv. Radiation Oncol.* **8**, 101159 (2023).
48. Tang, D. et al. High-mobility Group box 1 is essential for mitochondrial quality control. *Cell Metabol.* **13**, 701–711 (2011).
49. Zhou, J. et al. Immunogenic cell death in cancer therapy: present and emerging inducers. *J. Cell. Mol. Med.* **23**, 4854–4865 (2019).
50. Ashrafizadeh, M., Farhood, B., Musa, A. E., Taeb, S. & Najafi, M. Damage-associated molecular patterns in tumor radiotherapy. *Int. Immunopharmacol.* **86**, 106761 (2020).
51. Zhu, M. et al. Immunogenic cell death induction by ionizing radiation. *Front. Immunol.* **12**, 705361 (2021).
52. Vaes, R. D., Hendriks, L. E., Vooijs, M. & De Ruysscher, D. Biomarkers of radiotherapy-induced immunogenic cell death. *Cells.* **10**, 930 (2021).
53. Wang, X. et al. Targeting STAT3 enhances ndv-induced immunogenic cell death in prostate cancer cells. *J. Cell. Mol. Med.* **24**, 4286–4297 (2020).
54. Bu, L. et al. STAT3 induces immunosuppression by upregulating PD-1/PD-L1 in HNSCC. *J. Dent. Res.* **96**, 1027–1034 (2017).
55. Yu, H., Kortylewski, M. & Pardoll, D. Crosstalk between cancer and immune cells: Role of STAT3 in the tumour microenvironment. *Nat. Rev. Immunol.* **7**, 41–51 (2007).
56. Wang, Y., Shen, Y., Wang, S., Shen, Q. & Zhou, X. The role of STAT3 in leading the crosstalk between human cancers and the immune system. *Cancer Lett.* **415**, 117–128 (2018).
57. Rébé, C. & Ghiringhelli, F. STAT3, a master regulator of anti-tumor immune response. *Cancers.* **11**, 1280 (2019).
58. Zerde, I. et al. STAT3 activity promotes programmed-death ligand 1 expression and suppresses immune responses in breast cancer. *Cancers.* **11**, 1479 (2019).
59. Sato, H., Okonogi, N. & Nakano, T. Rationale of combination of anti-PD-1/PD-L1 antibody therapy and radiotherapy for cancer treatment. *Int. J. Clin. Oncol.* **25**, 801–809 (2020).
60. Tesniere, A. et al. Immunogenic death of colon cancer cells treated with oxaliplatin. *Oncogene.* **29**, 482–491 (2010).
61. Fang, H. et al. TLR4 is essential for dendritic cell activation and anti-tumor t-cell response enhancement by DAMPs released from chemically stressed cancer cells. *Cell Mol. Immunol.* **11**, 150–159 (2014).

Acknowledgements

Not applicable.

Author contributions

S.J. Done the experiments, wrote the main manuscript text and prepared figures. A. KA, E. MA and A. M cooperated in data analyzing and experimental design. S. M and O. M supervised the project, analyzed data and edited the manuscript. All authors reviewed the manuscript.

Funding

This work was financially supported by Molecular Medicine Research Center, Tabriz University of Medical Sciences, Tabriz, Iran (IR.TBZMED.VCR.REC.1402.084) (Pazhoohan ID: 71943).

Declarations

Competing interests

The authors declare no competing interests.

Additional information

Supplementary Information The online version contains supplementary material available at <https://doi.org/10.1038/s41598-024-72697-1>.

Correspondence and requests for materials should be addressed to S.M. or O.M.

Reprints and permissions information is available at www.nature.com/reprints.

Publisher's note Springer Nature remains neutral with regard to jurisdictional claims in published maps and institutional affiliations.

Open Access This article is licensed under a Creative Commons Attribution-NonCommercial-NoDerivatives 4.0 International License, which permits any non-commercial use, sharing, distribution and reproduction in any medium or format, as long as you give appropriate credit to the original author(s) and the source, provide a link to the Creative Commons licence, and indicate if you modified the licensed material. You do not have permission under this licence to share adapted material derived from this article or parts of it. The images or other third party material in this article are included in the article's Creative Commons licence, unless indicated otherwise in a credit line to the material. If material is not included in the article's Creative Commons licence and your intended use is not permitted by statutory regulation or exceeds the permitted use, you will need to obtain permission directly from the copyright holder. To view a copy of this licence, visit <http://creativecommons.org/licenses/by-nc-nd/4.0/>.

© The Author(s) 2024